Intent Inference of Deceleration Maneuvers and Its Safety Impact Evaluation by Driving Simulator Experiments

Hironori Suzuki
Department of Robotics, Nippon Institute of Technology, Saitama, Japan
Email: viola@nit.ac.jp

Sho Wakabayashi
Department of Environment System Engineering, Graduate School of Nippon Institute of Technology, Saitama, Japan
Email: wakabayashi.sho@nit-trlab.net

Yoshitaka Marumo
Department of Mechanical System Engineering, Nihon University, Chiba, Japan
Email: marumo.yoshitaka@nihon-u.ac.jp

***Abstract*—Though the autonomous driving is becoming a key solution to mitigate rear-end collisions, the driving assistance such as Advanced Driving Assistance System (ADAS) is still required to support drivers to be aware of the risk of rear-end collisions. The authors have been developing the intent inference system that advises the appropriate deceleration timing to mitigate the collision risk with the preceding vehicle. The purpose of the system is to infer the intent of a vehicle ahead 1.5 s in advance of its driver's most likely action. The proposed system has been well evaluated through a driving simulator experiment and a car-following simulation in previous studies by the authors. However, the car-following simulation itself is not enough to identify the safety effect of the assistance system on a vehicle platoon of a convoy. In this paper, the safety impact of the proposed assistance system on the platooned vehicles was assessed using additional driving simulator experiments. Numerical analyses showed that the proposed assistance was significantly effective for the safety of multiple vehicles in the platoon including the assisted car itself.**

***Index Terms*—state estimation, intent inference, Collision avoidance, car-following, driver assistance; ADAS, driving simulator experiment**

I. Introduction

Rear-end collisions in longitudinal car-following situations occasionally cause severe multiple-collision accidents, especially in high-density and high-speed traffic conditions. In such situations, the use of an Autonomous Collision Avoidance System (ACAS), which is one of the active safety measures of Advanced Driver Assistance Systems (ADAS), may provide a solution. Instead of the direct vehicle control provided by an ACAS, an estimation (or prediction) of driver intentions, such as lane changing and intersection turning intentions, can also provide useful data for accident avoidance solutions [1]-[12]. In addition, numerous sophisticated algorithms have been proposed for safer traffic not only for assisted vehicles but also for following vehicles in multiple-vehicle platoons [13]-[22].

The authors have previously proposed an advisory system that infers a preceding car driver's deceleration intention 1.5 s in advance of its driver's most likely action [23] and reports it to the following car's driver through a windshield display (WSD) [24]. This system integrates an unscented Kalman filter (UKF) with a conventional car-following scheme that is hereafter referred to as the Gazis-Herman-Rothery (GHR) model. Previously conducted driving simulator experiments have shown that the assistance provided by the system is quite effective in reducing collision risks, even in high-deceleration scenarios [24]. In addition, we confirmed through traffic simulator experiments that this safety-related impact was propagated upstream the platoon [25]. In the traffic simulations, however, the car-following behavior including the deceleration maneuver was based on the constant and assumed parameters. The car-following simulation itself is not enough to identify the safety effect of the assistance system on a vehicle platoon of a convoy.

In this paper, assuming that there are two cars traveling behind an ego vehicle, we attempt to assess the safety impact of the proposed assistance system on the platooned vehicles using additional driving simulator experiments. The characteristics of how the safety impact is propagated upstream the platoon is investigated with and without the ego vehicle advisory.

II. Model Development

A. Outline of the Assistance System

We begin by considering multiple vehicles forming a platoon and traveling along a corridor, as shown in Fig. 1.

Manuscript received July 12, 2019; revised December 11, 2019.

doi: 10.18178/jtle.7.2.28-34

Let v_i and d_i denote the velocity and headway of the *i*-the vehicle, respectively. Assuming that the second vehicle is equipped with sensors to measure d_2, d_3, and v_2, the PF and UKF calculate the velocity and headway, v_1, v_2, v_3, d_2, and d_3, of all three cars preceding the host vehicle. Here, measurement variables $\mathbf{y}(k)$ are set to $\mathbf{y}(k) = [v_2, d_2, d_3]^T$, whereas the state variables are $\mathbf{x}(k) = [v_1, v_2, v_3, d_2, d_3]^T$. If all these variables are identified in real-time, the acceleration of the third vehicle, a_3, which is expected to occur a few seconds later can be predicted in advance by the well-known Gazis-Herman-Rothery (GHR) car-following model.

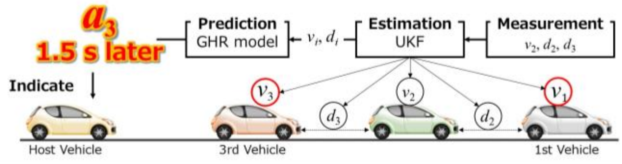

Figure 1. Outline of the assistance system

The GHR model is a conventional stimulus-response model that forecasts acceleration *T* steps ahead by using the current velocity and headway of both the preceding and pre-preceding cars at time *k*, as defined in equation (1).

$$
\begin{aligned}
a_i(k+T) &= \alpha w \frac{v_i{}^n}{d_i{}^m}\left(v_{i-1}-v_i\right)_{(k)} \\
&+ \alpha(1-w)\frac{v_i{}^n}{d_{i-1}{}^m + d_i{}^m}\left(v_{i-2}-v_{i-1}\right)_{(k)}
\end{aligned} \tag{1}
$$

Here, α, m, and n are sensitivity parameters and w ($0 \le w \le 1$) is a weight used to adjust the importance of the two preceding cars. If w is 1, the model considers the preceding car only. T is a vehicle reaction time.

If the predicted a_3 is reported to the following fourth (host) vehicle earlier than the third-car brake pedal operation is reported, the following driver is alert, and thus reacts much faster when the brake lights actually appear, thereby decreasing the risk of a rear-end collision. As the number of vehicles in the platoon increases, the collision risk reduction is reinforced along the entire platoon, so traffic becomes safer and more stable.

B. Modeling

v_1 and v_3, which cannot be measured directly by the second vehicle, are estimated by the UKF and PF. v_i is updated at each time step by the following differential equation:

$$
v_i(k) = \begin{cases} v_i(k-1) & (i=1) \\ v_i(k-1) + a_i(k-1)\Delta t & (i=2,3) \end{cases} \tag{2}
$$

Here, a_i is given by equation (1) and Δt is a time resolution. Headways d_2 and d_3 are defined by the conservation equation:

$$
d_i(k) = d_i(k-1) + \left[v_{i-1}(k-1) - v_i(k-1)\right]\Delta t \tag{3}
$$

One estimation problem is calculating the state variables $\mathbf{x}(k) = [v_1, v_2, v_3, d_2, d_3]^T$ from the measurements $\mathbf{y}(k) = [v_2, d_2, d_3]^T$. The state and measurement equations of a state-space model can be written in vector-matrix form as follows:

$$
\mathbf{x}_k = \mathbf{F}\left[\mathbf{x}_{k-1}, \mathbf{u}_{k-1}\right] + \mathbf{v}_{k-1}, \quad \mathbf{y}_k = \mathbf{G}\left[\mathbf{x}_k, \mathbf{u}_k\right] + \mathbf{n}_k \tag{4}
$$

where $\mathbf{u}_k$ is a known exogenous input and $\mathbf{v}_k$ and $\mathbf{n}_k$ are system and measurement noises. The function $\mathbf{F}$ is defined as equations (2) and (3), whereas $\mathbf{G}$ is the coefficients matrix.

C. UKF

The UKF is a *derivative-free* Kalman filter that does not require partial derivative calculations of the state and measurement equations [26]. The main UKF procedure is given in Table I. Let "^" and "~" denote the "filtered estimates" and "one-step time update", respectively. Then, the first step is to generate sigma point $\boldsymbol{\sigma}$ in order to calculate the time updates $\tilde{\mathbf{x}}_k$, $\tilde{\mathbf{y}}_k$ and the error

TABLE I. STATE FILTER BY UKF

(time update)

$$\boldsymbol{\sigma}_{i,P} = \left(\sqrt{(N+\lambda)\mathbf{P}_{k-1}}\right)_i \tag{5}$$

$$
\begin{aligned}
&\hat{\Phi}_{0,k-1} = \hat{\mathbf{x}}_{k-1}, \hat{\Phi}_{i,k-1} = \hat{\mathbf{x}}_{k-1} + \boldsymbol{\sigma}_{i,P}\ (i = 1,\ldots,N), \\
&\qquad \hat{\Phi}_{i,k-1} = \hat{\mathbf{x}}_{k-1} - \boldsymbol{\sigma}_{i-N,P}\ (i = N+1,\ldots,2N)
\end{aligned} \tag{6}
$$

$$\tilde{\boldsymbol{\Phi}}_k = \mathbf{F}\left(\hat{\boldsymbol{\Phi}}_{k-1}\right) \tag{7}$$

$$(\text{mean before measurement})\ \tilde{\mathbf{x}}_k = \sum_{i=0}^{2N} h_i \tilde{\Phi}_{i,k} \tag{8}$$

(variance before measurement)

$$\mathbf{M}_k^{xx} = \sum_{i=0}^{2N} h_i \left[\tilde{\Phi}_{i,k} - \tilde{\mathbf{x}}_k\right]\left[\tilde{\Phi}_{i,k} - \tilde{\mathbf{x}}_k\right]^T + \mathbf{Q}_k \tag{9}$$

$$h_i = \frac{1}{2(N+\lambda)} \tag{10}$$

$$\boldsymbol{\sigma}_{i,M} = \left(\sqrt{(N+\lambda)\mathbf{M}_k^{xx}}\right)_i \tag{11}$$

$$
\begin{aligned}
&\tilde{\Omega}_{0,k} = \tilde{\mathbf{x}}_0, \tilde{\Omega}_{i,k} = \tilde{\mathbf{x}}_k + \boldsymbol{\sigma}_{i,M}\ (i = 1,\ldots,N), \\
&\qquad \tilde{\Omega}_{i,k} = \tilde{\mathbf{x}}_k - \boldsymbol{\sigma}_{i,M}\ (i = N+1,\ldots,2N)
\end{aligned} \tag{12}
$$

$$\tilde{\boldsymbol{\Psi}}_k = \mathbf{G}\left(\tilde{\boldsymbol{\Omega}}_k\right) \tag{13}$$

$$\tilde{\mathbf{y}}_k = \sum_{i=0}^{2N} h_i \tilde{\Psi}_k \tag{14}$$

(measurement update)

$$\mathbf{M}_k^{yy} = \sum_{i=0}^{2N} h_i \left[\tilde{\Psi}_{i,k} - \tilde{\mathbf{y}}_k\right]\left[\tilde{\Psi}_{i,k} - \tilde{\mathbf{y}}_k\right]^T + \mathbf{R}_k \tag{15}$$

$$\mathbf{M}_k^{xy} = \sum_{i=0}^{2N} h_i \left[\tilde{\Phi}_{i,k} - \tilde{\mathbf{x}}_k\right]\left[\tilde{\Psi}_{i,k} - \tilde{\mathbf{y}}_k\right]^T \tag{16}$$

$$\mathbf{K}_k = \mathbf{M}_k^{xy}\left(\mathbf{M}_k^{yy}\right)^{-1} \tag{17}$$

$$(\text{mean after measurement})\ \hat{\mathbf{x}}_k = \tilde{\mathbf{x}}_k + \mathbf{K}_k\left(\mathbf{y}_k - \tilde{\mathbf{y}}_k\right) \tag{18}$$

$$(\text{variance after measurement})\ \mathbf{P}_k = \mathbf{M}_k^{xx} - \mathbf{K}_k \mathbf{M}_k^{xx} \mathbf{K}_k^T \tag{19}$$

covariance $\mathbf{M}_k^{xx}$ through sigma vectors $\mathbf{\Phi}_k$ and $\mathbf{\Omega}_k$. Here, N is the number of state variables, λ is a scaling parameter, and $\mathbf{Q}_k$ is the system error covariance. Next, covariance $\mathbf{M}_k^{yy}$ and $\mathbf{M}_k^{xy}$ are computed to obtain the Kalman gain $\mathbf{K}_k$. $\mathbf{R}_k$ is the covariance of the measurement error. It should be noted that equation (17) does not require the partial derivative calculation that must be performed in the conventional extended Kalman filter (EKF). This is why the UKF captures the posterior mean and covariance accurately by second-order Taylor expansions using a minimal set of carefully chosen sigma points. Finally, the expected mean $\hat{\mathbf{x}}_k$ and the variance $\mathbf{P}_k$ after the measurement are updated by (18) and (19).

III. Intent Inference of Deceleration Maneuvers

The driver's deceleration intent could be seen as a reflection of a vehicle's acceleration rate. After state variables $\mathbf{x}(k)$ are estimated through the UKF feedback processes, the prediction of acceleration rates $a_3(k+T)$ that are expected to occur T seconds later are given by equation (1).

A. Drving Simulator Experiment

A driving simulator (DS) experiments was carried out to collect data on a platoon consisted by the heavy vehicle (1st) and the following two passenger cars (2nd and 3rd) as shown in Fig. 2. In this set of experiments, six participants (P1– P6) were requested to drive the 3rd vehicle of the platoon and follow two preceding cars travelling on a straight corridor at 0 to 20 m/s with some acceleration and deceleration actions. In addition, they were instructed to maintain a headway distance that was close enough for them to read the four digits of the preceding car's license plate number. A heavy vehicle was used as the first car of the platoon, as it was important for the participants to recognize both preceding vehicles.

By examining the data collected through the DS experiment, the parameters of the GHR model are set as α=0.8, m=n=1, w=0.95, and T=1.5 s, while the time resolution Δt of the state estimator is set equal to 0.1 s. The covariance of errors $\mathbf{v}_k$ and $\mathbf{n}_k$ are set to 0.1 and 0.2 to 0.3, respectively. The scaling parameter λ in the UKF is 5.

B. Testing Results of Velocity and Headway Estimations

The estimator's performance was first examined for the v_1 and v_3 estimations by the UKF, which are the most important factors for the intent inference. Fig. 3 are the estimates of velocities for P1. It seems that the system is capable of tracking speed variations although they were not directly measured by the assistance system.

The other state variables such as v_2, d_2, and d_3 are directly measured, but contain measurement noises that should be eliminated through the estimator feedback processes. As depicted in Fig. 4, the UKF performed well for tracking the true measurements and filtering the noises.

For the six participants, the performance is summarized as root mean square errors (RMSEs) (Figure 5). The RMSE demonstrates that the UKF guarantees a satisfactory level of accuracy for all state variables.

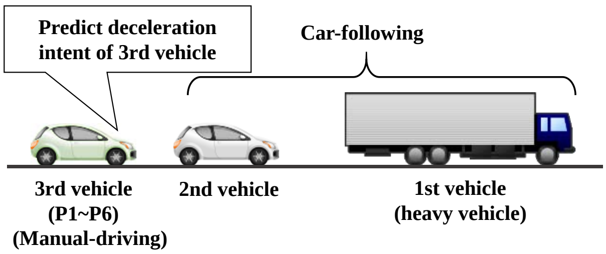

Figure 2. Three-vehicle convoy for a driving simulation experiment

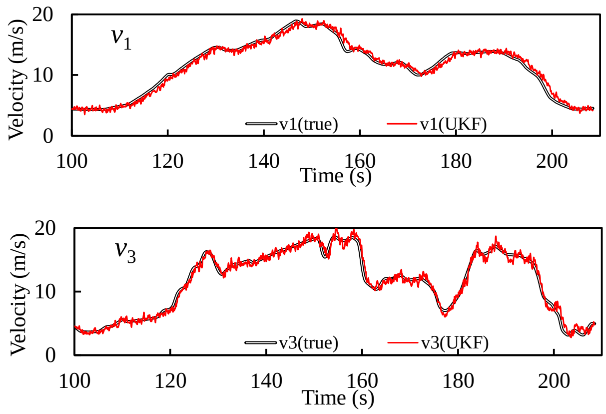

Figure 3. Velocity estimates for P1

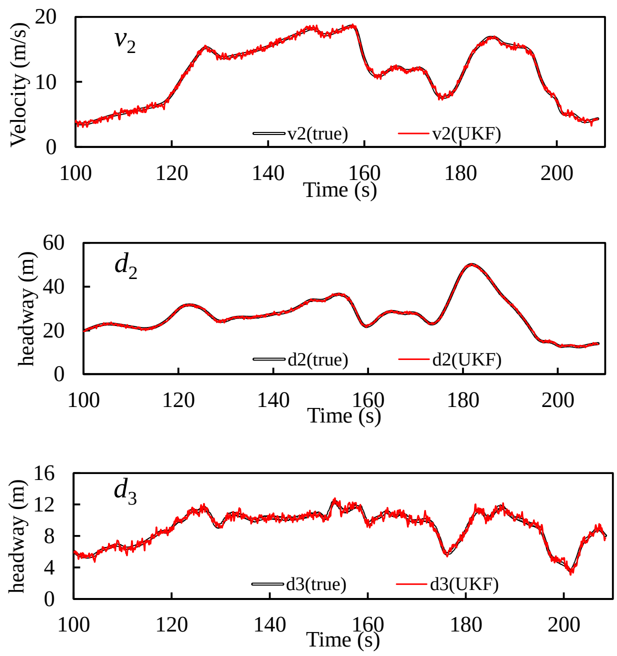

Figure 4. Estimates of state variables for P1

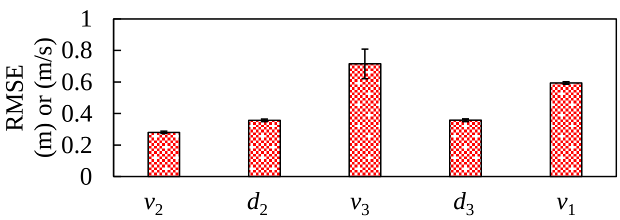

Figure 5. Errors of state estimations

C. Accuracy of Deceleration Intent

Fig. 6 illustrates the predicted deceleration of the 3rd vehicle for P1, P3 and P5 in which the prediction errors were 0.56, 0.73 and 0.93 m/s^2. The prediction did not completely match the actual measurement. However, the proposed system was capable of successfully inferring the driver's deceleration intention that is expected to occur 1.5 s later for both ordinary and emergency deceleration scenarios. The average error was less than 1 m/s^2.

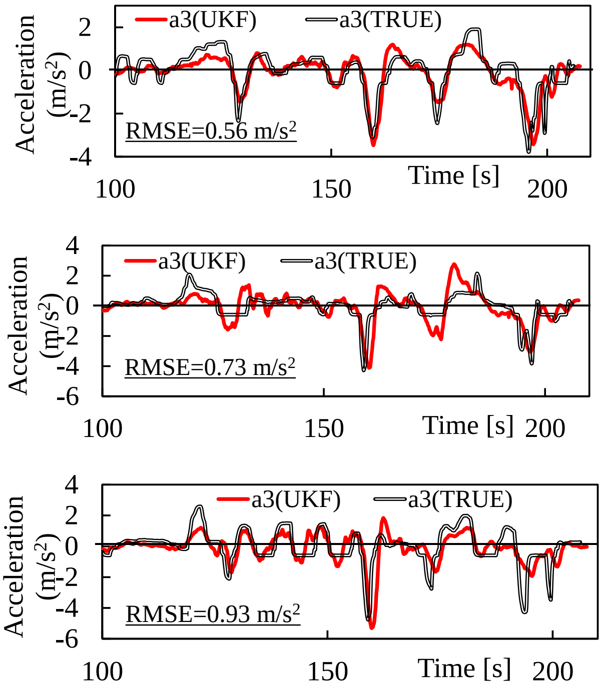

Figure 6. Accuracy of deceleration intent prediction

IV. Safety Impact of Intent Inference System

A. Interface

Since driver intentions contain high levels of behavior uncertainty, it is almost impossible to predict deceleration rates that precisely match the driver behaviors. Even if the inferred intent is not particularly accurate, it may provide valuable information for the following car driver and thus help mitigate collision risk. The key issue is not to attain absolutely accurate inference but to design an appropriate human machine interface (HMI) that reports the forecasted deceleration intent to the following car driver in a way that will assist in mitigating rear-end collisions, even though it will always contain some levels of uncertainty.

When reporting such unreliable information, they should be given to drivers in their peripheral vision in order to reduce their visual load. We therefore proposed a wind-shield-display (WSD) like interface that the colored bars appear from a pair of front pillars of a vehicle when necessary as shown in Fig. 7. The color changes depending on the amount of inferred deceleration from yellow, amber and red. Four regions are prepared such as "no intent", light, high and emergency deceleration intent. The boundaries between the regions are 0.05 G, 015 G and 0.25 G, respectively.

Figure 7. Interface design

The colored bars appear 1.5 s earlier than the actual deceleration of the preceding vehicle. Thus, the following driver is able to recognize in advance not only the timing of the deceleration onset but also the intensity of the deceleration. He or she reacts much faster when the brake lights actually appear, thereby decreasing the risk of a rear-end collision. As the number of vehicles in the platoon increases, the collision risk reduction is reinforced along the entire platoon, so traffic becomes safer and more stable.

B. Driving Simulator Experiment

A series of driving simulator (DS) experiments were carried out to evaluate the proposed driver assistance system. Seven participants (P7 to P13) were requested to drive the fourth vehicle of the platoon and another fifteen subjects (P14 to P28) were to maneuver the fifth and sixth cars when travelling on a 5-km straight corridor at 0 to 20 m/s with some acceleration and deceleration actions. Fig. 8 depicts the set-up of the DS experiment. The first three cars make a convoy and only the fourth vehicle is equipped with the WSD to assist P7 to P13.

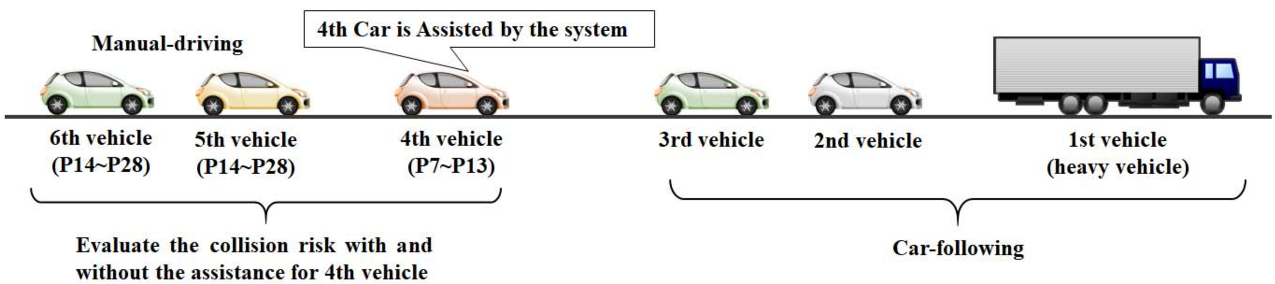

Figure 8. Set-up of a driving simulator experiment for system evaluation

The colored bar appears at least 1.5 seconds before the actual deceleration of the 3rd vehicle. The 5th and 6th vehicles, which are not assisted by the system are manual-driving cars. The risk of collision of the 4th to 6th cars were evaluated in terms of maximum deceleration (MDR) and minimum time-to-collision (TTC) with and without the assistance.

All participants were instructed to:

- Maintain a headway distance that was close enough for them to read the four digits of the preceding car's license plate number,
- Drive at an appropriate speed although there is no speed limit prepared,
- Make appropriate collision avoidance actions when necessary,
- Attempt to recognize the color bars in peripheral vision when they appear, i.e. concentrate on the preceding car(s) ahead to avoid collisions,
- Be noticed that the information given through the system was not always correct and there may be possibilities of malfunction and missed alarm.

In addition, they gave their informed consent before taking part in the experiment that was approved by the ethics committee of Nippon Institute of Technology.

C. *Test Conditions*

Enough numbers of pre-trial testing were carried out for the participants to adapt the driving by the DS with and without the assistance system given by the WSD. After that, two conditions were repeated twice; control condition (Condition I) and experimental condition with system (Condition II).

D. *Evaluation*

1) *4th vehicle*

As an example of the evaluation, the deceleration of P7 is shown in Fig. 9. Without the assistance, the MDR came to around 0.8 G at the emergency deceleration scenario. The proposed assistance, however, is able to reduce it until around 0.2 G. The mean and SD of the MDR and minimum TTC in total six participants (P7 to P13 except P11) are given in Figure 12. It is clear that the assistance significantly reduced the MSD ($t(22)$ = 4.083 ($p<0.01$)) and increased the minimum TTC ($t(22)$ = 3.520 ($p<0.05$)). This is due to the noteworthy effect of the system which induces the driver to be ready for the deceleration.

If the inferred deceleration is reported to the following vehicle earlier than the preceding-car brake pedal operation is reported, the following driver thus reacts much faster when a brake light actually appears, and the risk of a rear-end collision can be decreased.

2) *5th and 6th vehicles*

Fig. 10 and Fig. 11 are the comparisons of acceleration with and without the assistance for 4th vehicle. It was found that the effect of the assistance was gradually deteriorated as the shockwave is propagated through the platoon of vehicles. The performance of the manual-driving 5th and 6th vehicles was summarized as shown in Fig. 13 and Fig. 14. The MDR and minimum TTC were decreased and increased even though they are not equipped with the assistance system. In other words, even without equipped with the assistance system, the effect of risk mitigation is propagated from the assisted car to the following vehicles along the platoon. Not only the assisted vehicle but also the following cars are able to receive the benefit and thus the platoon becomes safer and more stable. However, the significance of the effect was gradually decreased as it is propagated upstream the platoon. The statistical significance was large ($t(10)$=3.759 ($p<0.01$) for MDR, $t(10)$= –4.455 ($p<0.01$) for TTC) if the 4th vehicle is firmly assisted.

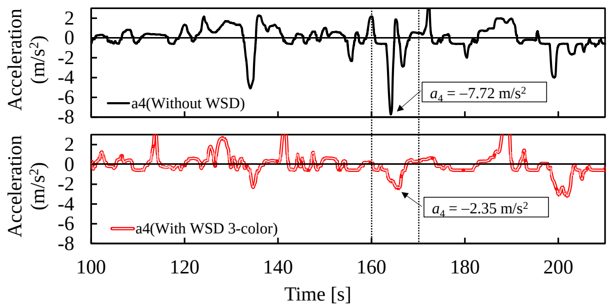

Figure 9. The acceleration with and without system (4th vehicle)

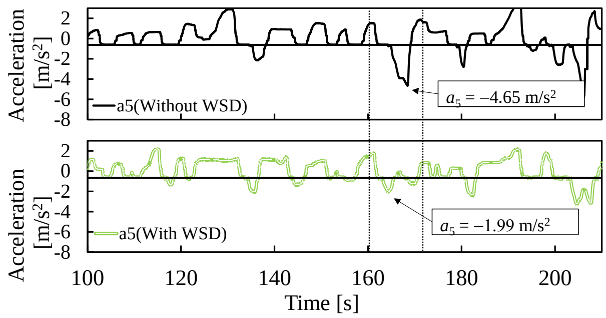

Figure 10. The acceleration with and without system (5th vehicle)

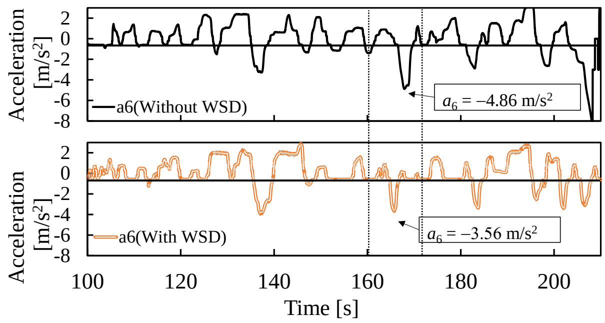

Figure 11. The acceleration with and without system (6th vehicle)

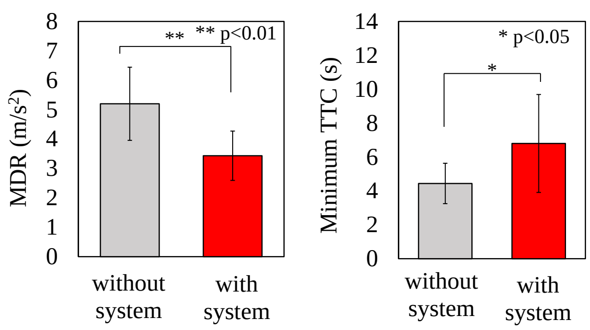

Figure 12. MDR and minimum TTC with and without system (4th Vehicle)

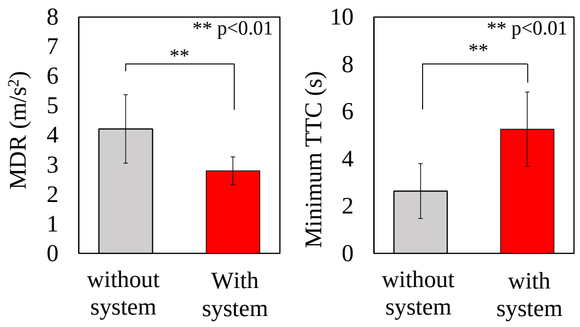

Figure 13. MDR and minimum TTC with and without system (5th Vehicle)

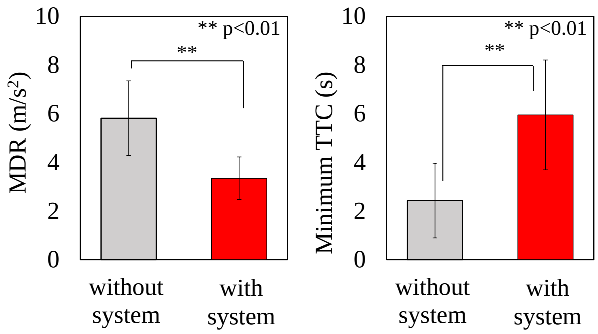

Figure 14. MDR and minimum TTC with and without system (6th Vehicle)

V. Conclusion

In this work, we developed the system that infers the deceleration behavior and reports it to the following vehicle at least 1.5 s earlier than the preceding-car brake pedal operation. We evaluated the proposed system to determine whether it is applicable not only in ordinary deceleration cases but also in scenarios where an emergency deceleration is required. Empirical results show that the system performed well in prediction of driver's deceleration intent.

We then designed a WSD like interface that reports the forecasted deceleration intent to the following car driver. A series of DS experiments showed that the system induced drivers to be ready for forthcoming braking of preceding car and reduced the effort of deceleration to avoid a collision. It was found that if the inferred deceleration is reported to the following vehicle earlier than the preceding-car brake pedal operation is reported, the following driver thus reacts much faster when a brake light actually appears, and the risk of a rear-end collision is decreased. In addition, the effect of risk mitigation is propagated from the assisted car to the following two vehicles along the platoon. Not only the assisted vehicle but also the following car are able to receive the benefit and thus the platoon becomes safer and more stable. However, it is also true that the significance of the effect was gradually decreased as it is propagated upstream the platoon.

In further research effort, the interface should be improved to a more sophisticated one and the proposed assistance system should be tested in various environment including high-speed and dense traffic on expressways or arterial roads.

Acknowledgment

This work was supported by the Japan Society for the Promotion of Science (JSPS) KAKENHI Grant Number 19K04926.

References

[1] J. C. McCall, D. P. Wipf, M. M. Trivedi, and B. D. Rao, "Lane change intent analysis using robust operators and sparse bayesian learning," *IEEE Trans. on Intelligent Transportation Systems*, vol. 8, no. 3, pp. 431–440, 2007.

[2] A. Doshi and M. Trivedi, "A comparative exploration of eye gaze and head motion cues for lane change intent prediction," in *Proc. IEEE Intelligent Vehicles Symposium*, 2008, pp. 49–54.

[3] A. Doshi and M. Trivedi, "On the roles of eye gaze and head dynamics in predicting driver's intent to change lanes," *IEEE Transactions on Intelligent Transportation Systems*, vol. 10, no. 3, pp. 453–462, 2009.

[4] A. Doshi and M. Trivedi, "Investigating the relationships between gaze patterns," in *Proc. Dynamic Vehicle Surround Analysis, and Driver Intentions, Intelligent Vehicles Symposium*, 2009, pp. 887–892.

[5] D. D. Salvucci, "Inferring driver intent: A case study in lane-change detection," in *Proc. Human Factors Ergonomics Society 48th Annual Meeting*, 2004.

[6] J. Gunnarsson, L. Svensson, E. Bengtsson, and L. Danielsson, "Joint driver intention classification and tracking of vehicles," in *Proc. Nonlinear Statistical Signal Processing Workshop*, 2006 IEEE, 2006, pp. 95–98.

[7] G. S. Aoude, V. R. Desaraju, L. H. Stephens, and J. P. How, "Driver behavior classification at intersections and validation on large naturalistic data set," *IEEE Trans. on Intelligent Transport Systems*, vol. 13, no. 2, pp. 724–736, 2012.

[8] T. Kumagai and T. Akamatsu, "Prediction of human driving behavior using dynamic bayesian network," *IEICE Trans. of Inf. & Syst.*, vol. E89-D, no. 2, pp. 857–860, 2006.

[9] R. Mabuchi and K. Yamada, "Prediction of driver's stop or go at yellow traffic signal from vehicle behavior," in *Proc. IEEE Intelligent Vehicles Symposium*, 2013, pp. 1161–1166.

[10] M. Liebner, M. Baumann, F. Klanner, and C. Stiller, "Velocity-based driver intent inference at urban intersections in the presence of preceding vehicles," *Intelligent Transportation Systems Magazine Summer*, pp. 10–21, 2013

[11] K. Lidstrom and T. Larsson, "Model-based estimation of driver intentions using particle filtering," in *Proc. 11th International IEEE Conference on Intelligent Transportation Systems*, 2008, pp. 1177–1182.

[12] Y. Saito, N. Hashimoto, S. Tsugawa, and S. Kato, "Development of deceleration intention indicating system of forward vehicle: Effect of the system," in *Proc. 15th International IEEE Conference on Intelligent Transportation Systems*, 2012, pp. 852–857.

[13] L. Li, G. Lu, Y. Wang, and D. Tian, "A Rear-end collision avoidance system of connected vehicles," in *Proc. IEEE 17th International Conference on Intelligent Transportation Systems*, 2014, pp. 63–68.

[14] W. Wang, W. Zhang, and H. Bubb, "Car-following safety algorithms based on adaptive cruise control strategies," in *Proc. SISY 2007, 5th International Symposium on Intelligent Systems and Lnformatics*, 2007, pp. 135–140.

[15] L. Xu and L. Y. Wang, G. Yin, and H. Zhang, "Coordinated control and communication for enhanced safety of highway vehicle platoons," in *Proc. International Conference on Connected Vehicles and Expo*, 2013, pp. 43–47.

[16] A. Mihaly, B. Nemeth, and P. Gaspar, "Enhancement of safety and economy of the vehicle platoon with the consideration of delays and disturbances," in *Proc. 12th IEEE International Symposium on Computational Intelligence and Informatics*, 2011, pp. 167–172.

[17] C. Guo, N. Wan, S. Mita, and M. Yang, "Self-defensive coordinated maneuvering of an intelligent vehicle platoon in

mixed traffic," in *Proc. 15th International IEEE Conference on Intelligent Transportation Systems*, 2012, pp. 1726–1733.
[18] X. Y. Lu and J. Wang, "Multiple-vehicle longitudinal collision avoidance and impact mitigation by active brake control," in *Proc. Intelligent Vehicles Symposium*, 2012, pp. 680–685.
[19] J. Wang, L. Zhang, D. Zhang, and K. Li, "An adaptive longitudinal driving assistance system based on driver characteristics," *IEEE Transactions on Intelligent Transportation Systems*, vol. 14, no. 1, March 2013, pp. 1–12, 2013.
[20] B. van Arem, C. J. G. van Driel, and R. Visser, "The impact of cooperative adaptive cruise control on traffic-flow characteristics", *IEEE Transactions on Intelligent Transportation Systems*, vol. 7, no. 4, December 2006, pp. 429–436.
[21] A. Kostikj, M. Kjosevski, and L. Kocarev, "Harmonized traffic stream in urban environment based on adaptive stop&go cruise control and its impact on traffic flow," in *Proc. IEEE International Conference on Vehicular Electronics and Safety*, 2012, pp. 140–145.
[22] J. Zhao, M. Oya, and A. E. Kamel, "A safety spacing policy and its impact on highway traffic flow," in *Proc. IEEE Intelligent Vehicles Symposium*, 2009, pp. 960–965.
[23] H. Suzuki, T. Ishikura, and Y. Marumo, "Intent inference of driver's deceleration behavior to mitigate risk of rear-end collision," in *Proc. Road Safety & Simulation International Conference*, 2017.
[24] H. Suzuki, T. Ishikura, and Y. Marumo, "Mitigation of rear-end collision risk based on intent inference of preceding car's deceleration behavior," in *Proc. 2nd IEEE International Conference on Intelligent Transportation Engineering*, 2017, pp. 194–197.
[25] H. Suzuki and T. Izawa, "Intent inference of driver's deceleration maneuver and its safety impact on a platoon of vehicles," in *Proc. 3rd IEEE International Conference on Intelligent Transportation Engineering*, 2018, pp. 287–290.
[26] S. Haykin, *Kalman Filtering and Neural Networks*, John Wiley & Sons, 2001.

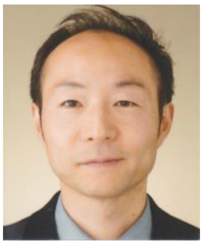

Hironori Suzuki received Doctor of Engineering in transportation engineering from Asian Institute of Technology, Bangkok, Thailand in 2001. After serving for Japan Automobile Research Institute (JARI) as a researcher, he joined the Faculty of Engineering, Nippon Institute of Technology as an assistant professor. He is currently teaching at Department of Robotics in Nippon Institute of Technology as a professor. His research interests are modelling of traffic systems, traffic simulation, active safety measures and driver assistance systems.

Sho Wakabayashi received his Bachelor of Engineering from Nippon Institute of Technology in 2019. He is currently a graduate student of department of environment system engineering, Nippon Institute of Technology, Japan.

Yoshitaka Marumo received B. Eng., M. Eng. and Dr. Eng. Degrees in Mechanical Systems Engineering from Tokyo University of Agriculture and Technology in 1998, 2000 and 2006 respectively. In 2000, he joined the Japan Automobile Research Institute (JARI). Since 2005, he has been with the College of Industrial Technology, Nihon University, where he is currently an Associate Professor. His research interests include driver assistance systems, and vehicle dynamics and control. He is a member of the Japan Society of Mechanical Engineers, Society of Automotive Engineers of Japan, the Society of Instrument and Control Engineers, and Human Interface Society.